Chemistry–A European Journal
Research Article
doi.org/10.1002/chem.202201660
Chemistry Europe
European Chemical Societies Publishing
www.chemeurj.org

Noncovalent Interactions Involving Group 6 in Biological Systems: The Case of Molybdopterin and Tungstopterin Cofactors

Antonio Bauzá*[a] and Antonio Frontera*[a]

Abstract: In this study we propose to coin the term Wolfium bond (WfB) to refer to a net attractive force (noncovalent interaction) between any element of group 6 and electron donor atoms (neutral molecules or anions) and to differentiate it from a coordination bond (metal-ligand interaction). We provide evidence of the existence of this interaction by inspecting the X-ray crystal structure of proteins containing Molybdopterin and Tungstopterin cofactors from the Protein Data Bank (PDB). The plausible biological role of the interaction as well as its physical nature (antibonding Wf-Ligand orbital involved) are also analyzed by means of *ab initio* calculations (RI-MP2/def2-TZVP level of theory), Atoms in Molecules (AIM), Natural Bond Orbital (NBO) and Noncovalent Interactions plot (NCIplot) analyses.

The wide range of possibilities that σ-hole interactions[1] (mainly composed by halogen, chalcogen, pnictogen and tetrel bonds) offer to chemical biologists, supramolecular chemists and crystal engineers in the past years has encouraged the investigation of novel noncovalent interactions (NCIs) by means of the inspection of structural databases and theoretical calculations.[2,3] These exploratory studies[4] have indeed facilitated the posterior experimental exploitation of NCIs in several fields of research (e.g., solid state chemistry, catalysis, enzymatic chemistry or materials science).[5]

Recently, scientists have tried to expand the σ-hole concept from the p-block to the transition metal block of elements (groups 3 to 12). In this context, several new NCIs have been theoretically proposed and experimentally exploited, such as regium/coinage bonding[6] (RgB) and spodium bonding[7] interactions (SpB), which refer to electron-deficient sites on a coinage-metal atom (group 11) and a spodium atom (group 12) and an electron donor molecule, respectively. Also, very recently, the terms "matere bond"[8] and "osme bond"[9] have been used to describe the attractive interaction between elements from groups 7 and 8 of the periodic table and electron donors, respectively.

Herein we propose to coin the term "Wolfium bond" to describe the net attractive force between an element of group 6 (see Figure 1) and an electron donor specie. The name Wolfium was inspired by the word wolfram, which derives from the German word "wolf rahm", that was how wolframite (a natural source of Wolframium) was traditionally known by the saxon miners.

Similarly to RgBs and SpBs, which have been characterized in a biological context,[10] we report evidence of this novel NCI in the context of Mo and W enzymatic chemistry by combining a search in the Protein Data Bank (PDB)[11] with an ab initio study at the RI-MP2/def2-TZVP level of theory to further demonstrate the existence and favorable nature of the interaction.

Our starting point was a PDB search where we looked for Mo and W protein-ligand complexes that could offer evidence of noncovalent binding with electron-rich species. To achieve that we considered X-ray crystal structures involving tetra- (WfX_4) and penta-coordinated (WfX_5) (Wf = Mo and W) sites that were establishing a noncovalent contact with an electron-rich specie = N, O and S, as is detailed in the Electronic Supporting

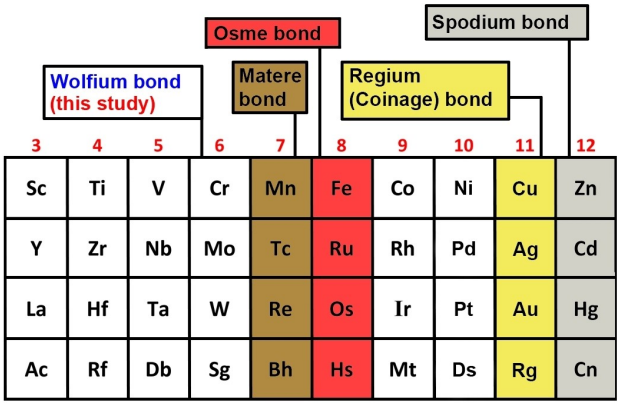

Figure 1. Donor-acceptor interactions involving the transition metal block of elements. Wolfium bond (group 6) is the name proposed in this work.

[a] *Prof. A. Bauzá, Prof. Dr. A. Frontera*
Departament de Química
Universitat de les Illes Balears
Ctra. de Valldemossa km 7.5, 07122 Palma de Mallorca (Baleares) (Spain)
E-mail: antonio.bauza@uib.es
toni.frontera@uib.es

Supporting information for this article is available on the WWW under https://doi.org/10.1002/chem.202201660

Information. We found 33 structures that were manually inspected to classify the interaction as either a noncovalent bond or a classical metal-ligand coordination bond. Two selected examples from the search are discussed below.

The first structure (PDBID 1AOR)[12] corresponds to a tungstopterin enzyme, which belongs to the family of aldehyde ferredoxin oxidoreductases (see Figure 2) from *Pyrococcus furiosus*. This protein reversibly oxidizes aldehydes to their corresponding carboxylic acids with the accompanying reduction of the redox protein ferredoxin at an optimally temperature of 100 °C. Its structure is composed by two identical subunits containing a W cofactor and a Fe_4S_4 cluster (see Figure 2a).

As noted in Figure 2(a), the tungstopterin cofactor is solely composed by the coordination to W(IV) of two PT molecules through four dithiolene groups in a distorted square pyramid fashion, showing an angle between the planes of the PT ligands of around 97 degrees. In addition, the two PT (pterin) ligands are also linked through their phosphate groups, which occupy the axial positions of an octahedral Mg^{2+} coordination complex. The coordination sphere of this Mg ion is fulfilled by two water molecules and two carbonyl oxygens belonging to residues ASN93 and ALA183 (not shown in Figure 2a).

Interestingly, the side chain of GLU313 is in the vicinity of the substrate binding site (near the W center) and might be involved in proton transfer reactions associated with the oxidation-reduction mechanism. This residue is involved in a noncovalent contact (O···Mo distance of 3.458 Å and O···W–S angle of 165.9°) with the WS_4 coordination complex. The computed interaction energy of this "Wolfium bond" (WfB) at the RI-MP2/def2-TZVP level of theory resulted in −15.6 kcal mol^{-1}, which is a moderately strong value. We also calculated the strength of the WfB in the absence of the Mg ion, resulting in −14.8 kcal mol^{-1}, which points to a long-range reinforcement of the WfB upon the formation of the Mg octahedral center. The favorable interaction energy values obtained can be attributed to electrostatics, since the Molecular Electrostatic Potential (MEP) surface of the W center indicates the presence of two positive regions (see Figure 2b) which correspond to the two vacant coordination positions of the W center. These positive electrostatic potential regions are located along the extension of the W–S bonds, resembling the concept of a σ-hole.[13] In addition, we performed an "Atoms in Molecules" (AIM)[14] analysis to this system (see Figure S1a in the Supporting Information), revealing a bond critical point (BCP) and a bond path connecting both the O-GLU_{313} and the W atoms, therefore characterizing the WfB interaction. The favorable nature of the interaction was also reflected in the Non Covalent Interactions plot (NCIplot)[15] analysis, which is a visual index that accounts for the nature and location of NCIs in real space. In this regard, we found a green reduced density gradient (RDG) isosurface between the O and W atoms (see also Figure S1a in the Supporting Information), therefore confirming the weak nature of the interaction. Finally, in Figure 2(a) we included the Natural Bond Orbital (NBO)[16] analysis of the WfB complex to investigate possible orbital donor-acceptor interactions in this system. We found two main orbital contributions that involve the donation from a lone pair (LP) of the oxygen atom to i) an unfilled p orbital of the W atom and ii) to a σ antibonding (σ-BD*) orbital of the W–S bond, with magnitudes of 2.7 and 4.1 kcal mol^{-1}, respectively. Interestingly, the involvement of the W–S antibonding orbital resembles that of the σ-hole family of interactions (e.g., Halogen (Hal) and Chalcogen (Ch) bonds), where Hal-X and Ch–X σ antibonding orbitals are also involved.

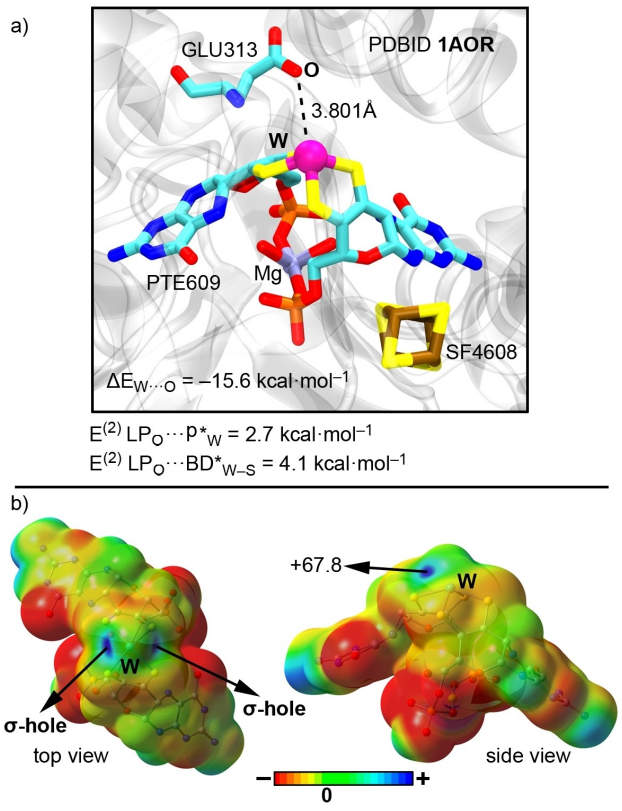

Figure 2. a) X-ray structure of PDBID 1AOR. b) MEP (Molecular Electrostatic Potential) surface of the Tungstopterin cofactor. The energy value is given in kcal mol^{-1} (0.001 a.u.).

The second example (PDBID 1FFV)[17] corresponds to the structure of a carbon monoxide dehydrogenase (CODH), present in *Hydrogenophaga pseudoflava*. Its active site presents a Mo(VI) ion coordinated by two dithiolate groups from a PT cofactor and three non-protein O-ligands (two oxo groups and a water molecule, see Figure 3) in a distorted square pyramidal coordination geometry. In their study, the authors focused their attention on the GLU757 side chain, concluding that the interaction with the Mo ion conditioned to some extent the position of this catalytic residue, while the position of other residues also present in the protein active site (such as GLN237 and ARG384) remained unchanged.

As noticed in Figure 3, a "Wolfium bond" (WfB) is undertaken between an O atom from the carboxylate group of GLU757 and the Mo(VI) cofactor (O···Mo distance of 3.801 Å and O···Mo–O_w angle of 159.4°), with an interaction energy value of −9.0 kcal mol^{-1}. Similarly, to the example discussed above, we performed a MEP surface analysis on the Mo cofactor, which indicated the presence of a positive electrostatic potential

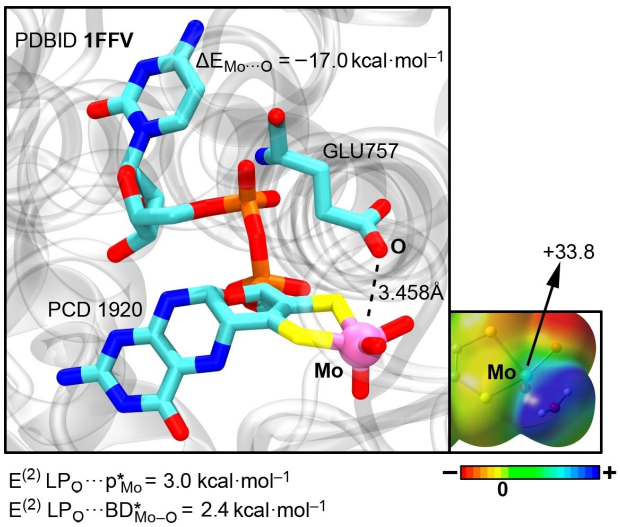

Figure 3. X-ray structure of PDBID 1FFV and partial MEP surface (0.001 a.u.) of a Molybdopterin cofactor. The MEP value at the Mo σ-hole is given in kcal mol^{-1}.

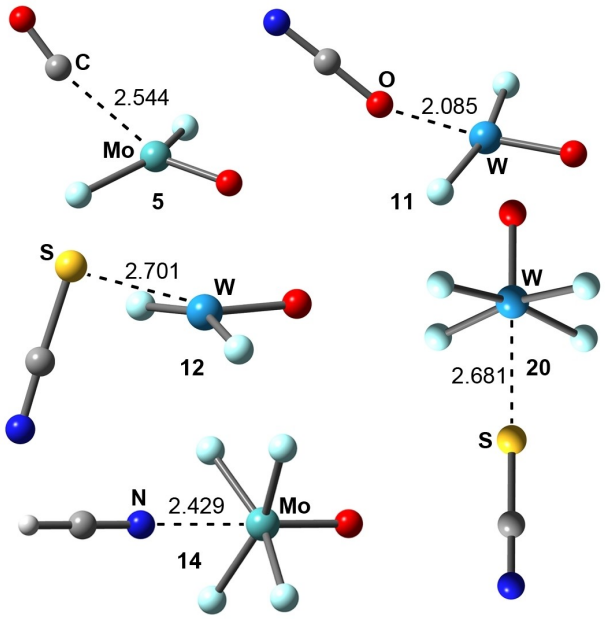

Figure 5. Optimized geometries of some representative WfB complexes (**5**, **11**, **12**, **14** and **20**) at the RI-MP2/def2-TZVP level of theory.

region on the extension of the axial Mo–O coordination bond. Furthermore, the NBO analysis also revealed two main orbital contributions responsible for the stabilization of the non-covalent complex, which also involved a σ-antibonding Mo–O orbital (with a magnitude of 2.4 kcal mol^{-1}). Lastly, the NCIplot analysis (see Figure S1b in the Supporting Information) revealed the presence of a green isosurface between the O atom from the carboxylate group and the Mo atom, thus confirming the presence of the WfB.

To rationalize these findings, the interaction energies between electron donating (lone-pair containing) molecules (CO, NCH, OCN^- and SCN^-) with compounds **1**–**4** were computed at the RI-MP2/def2-TZVP level of theory (see Figures 4 and 5). Compounds **1** to **4** were built on the basis of studying noncovalent interactions in neutral Wf(IV) and Wf(VI) coordination environments and preventing the valence expansion of the metal atom. The results of these calculations are gathered in Table 1.

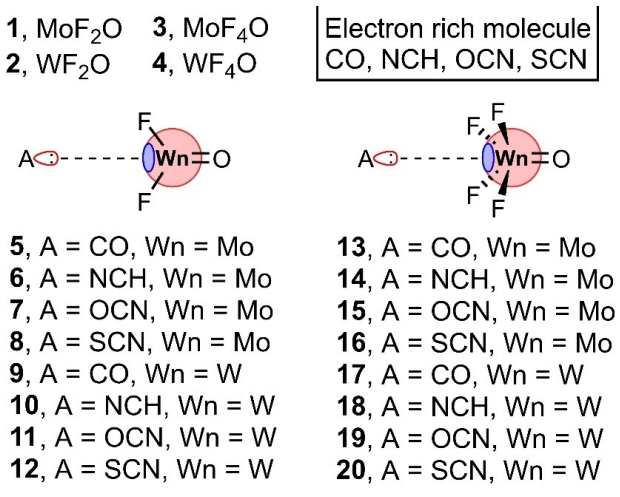

Figure 4. Compounds **1** to **4** and complexes **5** to **20** used in this study.

As noted, the interaction energies are in all the cases attractive and range from weak (−4.0 kcal mol^{-1} for complex **5**) to strong (−45.6 kcal mol^{-1} for complex **19**). In general, those complexes involving neutral electron donors (CO and HCN, complexes **5**, **6**, **9**, **10**, **13**, **14**, **17** and **18**) achieved weaker interaction energy values than those involving the anionic species (OCN^- and SCN^-, complexes **7**, **8**, **11**, **12**, **15**, **16**, **19** and **20**), as expected. Complexes **6**, **7**, **8**, **11**, **15** and **19** exhibit equilibrium distances slightly below the sum of the covalent radii between Mo/W and A (A = C, O, N and S), thus likely indicating that the minima found in these cases represented a classical ligand-Metal bond. On the other hand, in the rest of the complexes studied the equilibrium distances obtained lied between the sum of the covalent and vdW radii, suggesting a noncovalent interaction.

Table 1. RI-MP2/def2-TZVP BSSE corrected energies (ΔE_{BSSE}, kcal mol^{-1}), equilibrium distances (d in Å and in parenthesis) and value of the density at the bond critical point (BCP) of WfB complexes **5**–**20**. The complexes highlighted in orange are shown in Figure 5.

Complex	ΔE (d) $\rho\times100$	Complex	ΔE (d) $\rho\times100$
5 (CO···**1**)	−4.0 (2.544) 3.63	**13** (CO···**3**)	−8.2 (2.599) 3.49
6 (HCN···**1**)	−13.0 (1.991) 11.14	**14** (HCN···**3**)	−13.7 (2.429) 4.30
7 (CNO···**1**)	−32.5 (2.085) 10.24	**15** (CNO···**3**)	−40.5 (2.076) 8.50
8 (NCS···**1**)	−31.4 (2.479) 8.10	**16** (NCS···**3**)	−14.2 (2.652) 3.67
9 (CO···**2**)	−4.1 (2.673) 2.93	**17** (CO···**4**)	−8.9 (2.617) 3.57
10 (HCN···**2**)	−10.7 (2.465) 4.13	**18** (HCN···**4**)	−15.4 (2.431) 4.55
11 (CNO···**2**)	−44.9 (2.085) 9.01	**19** (CNO···**4**)	−45.6 (2.083) 8.74
12 (NCS···**2**)	−31.5 (2.701) 5.19	**20** (NCS···**4**)	−17.4 (2.681) 3.70

Among complexes involving WfF_2O (Wf = Mo and W) (**5** to **12**), adducts **5** and **9** involving CO as electron donor achieved a similar interaction energy value (−4.0 and −4.1 kcal mol^{-1}, respectively). On the other hand, in the case of complexes involving HCN (**6** and **10**), the former exhibited a stronger interaction energy value (−13.0 kcal mol^{-1}). Finally, among complexes with OCN^- and SCN^- anions (**7**, **8**, **11** and **12**), those involving the former anion achieved larger interaction energy values (complex **7**, −32.5 kcal mol^{-1} and complex **11**, −44.9 kcal mol^{-1}), likely due to the shorter distance (O is smaller than S).

In the case of complexes involving WfF_4O (W = Mo and W) (**13** to **20**), those with WF_4O (**17** to **20**) achieved larger interaction energy values than their corresponding MoF_4O analogous (**13** to **16**).

Despite of this, the differences in strength between the Mo and W sets of complexes are modest (from 0.5 to 2 kcal mol^{-1} among neutral WfB complexes and from 3 to 5 kcal mol^{-1} for anionic complexes). Among the neutral bases used, complexes **14** and **18** involving HCN achieved larger interaction energy values (−13.7 and −15.4 kcal mol^{-1}) (shorter equilibrium distances) compared to those involving sp C atoms (**13** and **17**).

On the other hand, for complexes involving the anionic electron donors (**15**, **16**, **19** and **20**) those involving O as electron donor resulted in more favorable interaction energy values (complex **15**, −40.5 kcal mol^{-1} and complex **19**, −45.6 kcal mol^{-1}), in line with the results obtained for the WfF_2O moiety. Interestingly, the values of the interaction energy obtained involving neutral electron donors lied within the same range than those obtained for neutral Osme bond[9] and Spodium bond complexes.[7]

To rationalize these results from an electrostatic point of view we performed the MEP surfaces of compounds **1** to **4** (see Figure 6). As noticed, in all four compounds an electrophilic region (positive electrostatic potential value) can be observed along the vector of the Wf=O bond, which resembles that for the classical and well-known σ-hole interactions observed p-block elements.[13] In addition, the MEP value obtained for compound **2** is more positive than that in **1**, in agreement to that observed for σ-hole based interactions. On the contrary, among both WfF_4O derivatives (compounds **3** and **4**) the opposite behavior was observed, being the MEP value of compound **3** slightly more positive than that for compound **4**. Similar behavior was observed in Spodium bonds,[7] where it was demonstrated that Cd is more prone to participate in SpBs than Hg.

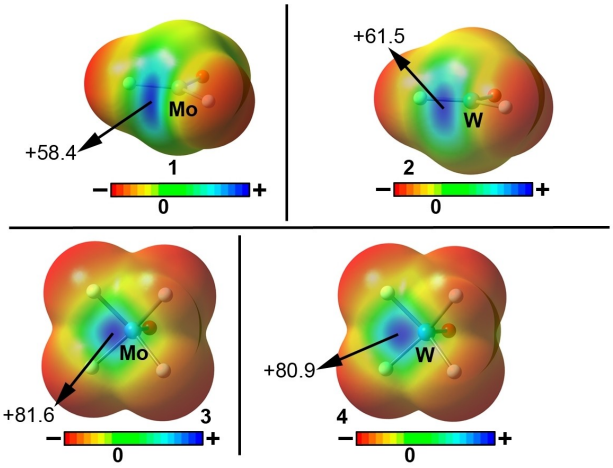

Figure 6. MEP (Molecular Electrostatic Potential) surfaces of compounds **1** to **4**. The energies highlighted at selected points in the surface are given in kcal mol^{-1} (0.001 a.u.).

To further understand the nature of the interaction, Natural Bond Orbital analysis[16] (see Supporting Information for additional examples) has been also used to investigate possible orbital donor-acceptor interactions in the noncovalent complexes studied herein by using the second order perturbation analysis. The results for some representative complexes are summarized in Table 2 revealing an orbital stabilization that comes from the donation of i) a lone pair (LP) of the electron-rich atom (O and S) or ii) a C–N bonding (BD) orbital to a σ antibonding (BD*) Wf–O orbital, with values ranging from 1.7 to 13.4 kcal mol^{-1}). This type of orbital stabilization helps to differentiate WfBs from coordination bonds, where d-orbitals of the metal are usually involved. Besides, in complexes **11** and **12** an additional orbital interaction involving a LP from the electron-rich moiety to an unfilled d orbital from the metal atom was observed, with values of 6.7 and 8 kcal mol^{-1}, respectively. The presence of this additional orbital contribution likely indicates that the binding mode present in these two complexes lies between a noncovalent interaction and a coordination bond, in agreement with the short intermolecular distances observed (see Table 1).

We have also used Bader's AIM Theory[14] to analyze the complexes studied herein from a charge-density perspective. The results show the presence of an intermolecular bond critical point (BCP) between the interacting molecules. In Figure 7, a selection of complexes is shown to provide a representative example of each donor-acceptor system used. As noted, in all the cases only one BCP and a bond path were found between the electron-rich atom (N, S, C and O) and the Mo and W atoms, thus confirming the presence of a noncovalent contact.

The values of the charge density (ρ) at the BCPs are gathered in Table 1. Their range from 2.9×10^{-2} to 11.1×10^{-2} a.u., typical of noncovalent interactions and metal-ligand interactions.[19] The lowest value corresponds to complex **9** that presents the weakest WfB and longest distance. In general,

Table 2. Second order perturbation analysis ($E^{(2)}$, in kcal mol^{-1}) of WfB complexes **5**, **11**, **14**, **17** and **24** with indication of the donor and acceptor orbitals at the HF/def2-TZVP level of theory. LP, BD, BD*, p* and d* stand for lone pair, bonding orbital, antibonding orbital, unfilled p orbital and unfilled d orbital, respectively.

Complex	Donor	Acceptor	$E^{(2)}$
5 (CO···**1**)	LP O	BD* Mo–O	5.46
11 (OCN···**2**)	LP O	d* W	6.65
		BD* W–O	13.36
12 (NCS···**2**)	LP S	d* W	8.08
		BD* W–O	3.10
14 (HCN···**3**)	BD C-N	BD* Mo–O	1.70
20 (NCS···**4**)	LP S	BD* W–O	3.36

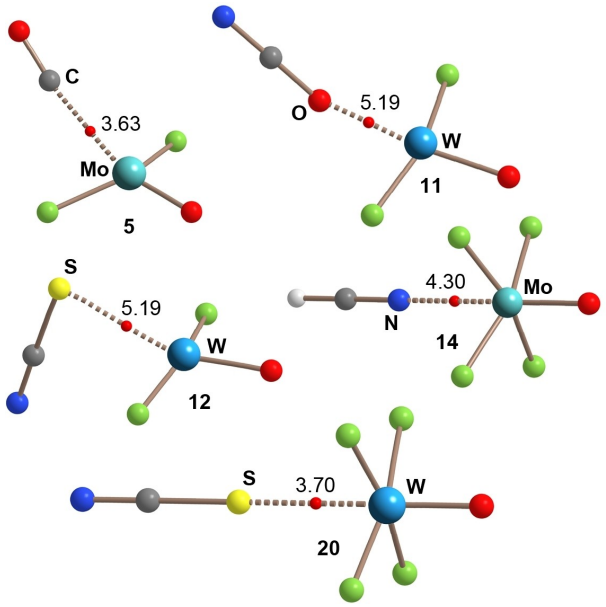

Figure 7. Distribution of CPs (bond CPs in red) and bond paths for WfB complexes (**5**, **11**, **12**, **14** and **20**). The value of the density at the bond CP is given in a.u. ($\rho \times 100$).

there is a good correlation between the WfB distances and the values of ρ (the shorter the distance the greater the ρ) in line with previous investigations.[8–10] Apart from complexes **6**–**8**, **11**, **15** and **19**, that exhibit equilibrium distances slightly below the sum of the covalent radii, the values of ρ at the BCP are similar to those reported for noncovalent interactions involving elements of groups 7[8] and 8.[9]

Concluding Remarks

In this work the name Wolfium bond (WfB) is proposed to describe the attractive interaction between elements from group 6 (mainly Mo and W) and electron-rich species. This name has been proposed to differentiate noncovalent interactions from classical coordination bonds (formation of ligand-Metal bond), in line with the recently proposed Osme and Spodium bonding interactions. Experimental evidence of this interaction was retrieved from the PDB, particularly from an X-ray crystal structure analysis involving Molybdopterin and Tungstopterin cofactors. The results were combined with an ab initio study at the RI-MP2/def2-TZVP level of theory and NBO, QTAIM and NCIplot methodologies were used to provide theoretical support for the existence of such interaction, which might help to advance in the rationalization and understanding of Molybdenum and Wolframium-dependent enzymes functions and properties as well as to continue expanding the σ-hole concept to new areas in chemistry and biology. We believe Wolfium bonds might be important contributors in the solid state of inorganic compounds as well as in small molecule organometallic catalysis. Further studies regarding those topics are currently under investigation and will be published in due course.

Computational Methods

General considerations: The energies of all complexes included in this study were computed at the RI-MP2/def2-TZVP[20] level of theory. Also, for Mo and W atoms, pseudopotentials along with the def2-TZVP basis set were used to accelerate the calculations and to account for relativistic effects, which cannot be neglected. The calculations have been performed by means of the program TURBOMOLE version 7.2.[21] using the supermolecule approximation, where the binding energy values (ΔE_{BSSE}) were calculated as the energy difference between the optimized structures of the complex and isolated monomers following the supermolecule approximation ($\Delta E_{complex} = E_{complex} - E_{monomerA} - E_{monomerB}$).

Calculating the strength of complexes 5 to 24: Complexes **5** to **24** (except for complex **14** involving WF_2O and SCN^-) were fully optimized imposing the Cs symmetry point group. In the case of complex **24** a potential energy surface relaxed scan was performed to find a noncovalent minimum, to avoid the formation of a W–S coordination bond.

Calculating the strength of biological assemblies: In the case of calculations regarding PDB X-ray structures, the H atoms were initially optimized at the BP86[22]-D3[23]/def2-SVP[20] level of theory while keeping the rest of the geometry frozen. In a later stage, the resulting geometry was used as starting point for single point calculations at the RI-MP2/def2-TZVP level of theory. Optimization of the whole geometry led to a different minimum where other noncovalent forces (e.g., hydrogen bond) or metal coordination dominated the assembly, therefore not being useful to investigate the noncovalent interactions presented herein.

NBO and AIM analyses: The topology of the electron density regarding complexes **5** to **24** as well as the selected biological assemblies has been analyzed within the Quantum Theory of Atoms in Molecules (QTAIM)[15] methodology by means of the AIMAll program[24] (using the RI-MP2 and B3LYP[25] methods, respectively). The non-covalent index (NCI)[15] of the protein assemblies (see Figure S1 in the Supporting Information) has been computed at the B3LYP[25] computational level using the Gaussian 16 program[26] and plotted with AIMall. Finally, the NBO analysis[16,27] has also been carried out using the Gaussian 16 calculation package at the HF computational level since it is not available at MP2 level.

Acknowledgements

We thank the MICIU/AEI (project PID2020-115637GB-I00 FEDER funds) for financial support. We thank the CTI (UIB) for computational facilities.

Conflict of Interest

The authors declare no conflict of interest.

Data Availability Statement

The data is available in the electronic supporting file or upon request to the authors

Keywords: ab initio study · chemical biology · non-covalent bonding · supramolecular chemistry · wolfium bond

[1] G. Cavallo, P. Metrangolo, T. Pilati, G. Resnati, G. Terraneo, *Cryst. Growth Des.* **2014**, *14*, 2697–2702.
[2] a) S. Scheiner, M. Michalczyk, W. Zierkiewicz, *Coord. Chem. Rev.* **2020**, *405*, 213136; b) A. Bauza, A. Frontera, *Coord. Chem. Rev.* **2020**, *404*, 213112; c) J. Y. C. Lim, P. D. Beer, *Chem.* **2018**, *4*, 731–783; d) M. H. Kolar, P. Hobza, *Chem. Rev.* **2016**, *116*, 5155–5187; e) A. Daolio, P. Scilabra, G. Terraneo, G. Resnati, *Coord. Chem. Rev.* **2020**, *413*, 213265.
[3] a) M. Fourmigué, A. Dhaka, *Coord. Chem. Rev.* **2020**, *403*, 213084; b) N. Biot, D. Bonifazi, *Coord. Chem. Rev.* **2020**, *413*, 213243; c) P. Scilabra, G. Terraneo, G. Resnati, *Acc. Chem. Res.* **2019**, *52*, 1313–1324; d) L. Vogel, P. Wonner, S. M. Huber, *Angew. Chem. Int. Ed.* **2019**, *58*, 1880–1891; *Angew. Chem.* **2019**, *131*, 1896–1907; e) K. Strakova, L. Assies, A. Goujon, F. Piazzolla, H. V. Humeniuk, S. Matile, *Chem. Rev.* **2019**, *119*, 10977–11005.
[4] a) P. Politzer, J. S. Murray, T. Clark, *Phys. Chem. Chem. Phys.* **2013**, *15*, 11178–11189; b) A. Bauza, T. J. Mooibroek, A. Frontera, *ChemPhysChem* **2015**, *16*, 2496–2517.
[5] a) J. Pascoe, K. B. Ling, S. L. Cockroft, *J. Am. Chem. Soc.* **2017**, *139*, 15160–15167; b) L. J. Riwar, N. Trapp, K. Root, R. Zenobi, F. Diederich, *Angew. Chem. Int. Ed.* **2018**, *57*, 17259–17264; *Angew. Chem.* **2018**, *130*, 17506–17512; c) M. Macchione, A. Goujon, K. Strakova, H. V. Humeniuk, G. Licari, E. Tajkhorshid, N. Sakai, S. Matile, *Angew. Chem. Int. Ed.* **2019**, *58*, 15752–15756; *Angew. Chem.* **2019**, *131*, 15899–15903; d) P. Wonner, A. Dreger, L. Vogel, E. Engelage, S. M. Huber, *Angew. Chem. Int. Ed.* **2019**, *58*, 16923–16927; *Angew. Chem.* **2019**, *131*, 17079–17083; e) W. Wang, H. Zhu, S. Liu, Z. Zhao, L. Zhang, J. Hao, Y. Wang *J. Am. Chem. Soc.* **2019**, *141*, 9175–9179; f) A. Borissov, I. Marques, J. Y. C. Lim, V. Félix, M. D. Smith, P. D. Beer, *J. Am. Chem. Soc.* **2019**, *141*, 4119–4129; g) S. Benz, M. Macchione, Q. Verolet, J. Mareda, N. Sakai, S. Matile, *J. Am. Chem. Soc.* **2016**, *138*, 29, 9093–9096; h) V. L. Heywood, T. P. J. Alford, J. J. Roeleveld, S. J. Lekanne Deprez, A. Verhoofstad, J. I. van der Vlugt, S. R. Domingos, M. Schnell, A. P. Davis, T. J. Mooibroek, *Chem. Sci.* **2020**, *11*, 5289–5293.
[6] a) J. H. Stenlid, A. J. Johansson, T. Brinck, *Phys. Chem. Chem. Phys.* **2018**, *20*, 2676–2692; b) J. H. Stenlid, T. Brinck, *J. Am. Chem. Soc.* **2017**, *139*, 11012–11015; c) A. Avramopoulos, M. G. Papadopoulos, A. J. Sadlej, *Chem. Phys. Lett.* **2003**, *370*, 765–769; d) M. Gao, Q. Li, H. B. Li, W. Li, J. Cheng, *RSC Adv.* **2015**, *5*, 12488–12497; e) Q. Li, H. Li, R. Li, B. Jing, Z. Liu, W. Li, J. Sun, *J. Phys. Chem. A* **2011**, *115*, 2853–2858; f) A. C. Legon, N. R. Walker, *Phys. Chem. Chem. Phys.* **2018**, *20*, 19332–19338.
[7] A. Bauzá, I. Alkorta, J. Elguero, T. J. Mooibroek, A. Frontera, *Angew. Chem. Int. Ed.* **2020**, *59*, 17482–17487; *Angew. Chem.* **2020**, *132*, 17635–17640.
[8] A. Daolio, A. Pizzi, G. Terraneo, A. Frontera, G. Resnati, *ChemPhysChem* **2021**, *22*, 2281–2285.
[9] A. Daolio, A. Pizzi, M. Calabrese, G. Terraneo, S. Bordignon, A. Frontera, G. Resnati, *Angew. Chem. Int. Ed.* **2021**, *60*, 20723–20727; *Angew. Chem.* **2021**, *133*, 20891–20895.
[10] a) H. S. Biswal, A. K. Sahu, A. Frontera, A. Bauzá, *J. Chem. Inf. Model.* **2021**, *61*, 3945–3954; b) M. N. Piña, A. Frontera, A. Bauzá, *J. Phys. Lett.* **2020**, *11*, 8259–8263.
[11] H. M. Berman, J. Westbrook, Z. Feng, G. Gilliland, T. N. Bhat, H. Weissig, I. N. Shindyalov, P. E. Bourne, *Nuc. Acids Res.* **2000**, *28*, 235–242.
[12] M. K. Chan, S. Mukund, A. Kletzin, M. W. W. Adams, D. C. Rees, *Science* **1995**, *267*, 1463–1469.
[13] A. Bauzá, T. J. Mooibroek, A. Frontera, *ChemPhysChem* **2015**, *16*, 2496–2517.
[14] R. F. W. Bader, *Chem. Rev.* **1991**, *91*, 893–928.
[15] E. R. Johnson, S. Keinan, P. Mori-Sánchez, J. Contreras-García, A. J. Cohen, W. Yang, *J. Am. Chem. Soc.* **2010**, *132*, 6498–6506.
[16] F. Weinhold, C. R. Landis, in *Valency and Bonding: A Natural Bond Orbital Donor-Acceptor Perspective*, Cambridge University Press, Cambridge, UK, **2005**.
[17] P. Hänzelmann, H. Dobbek, L. Gremer, R. Huber, O. Meyer, *J. Mol. Biol.* **2000**, *301*, 1221–1235.
[18] M. L. Kuznetsov *Int. J. Quantum Chem.* **2019**, *119*, e25869.
[19] a) R. Llull, G. Montalbán, I. Vidal, R. M. Gomila, A. Bauzá, A. Frontera, *Phys. Chem. Chem. Phys.* **2021**, *23*, 16888; b) P. Kumar, A. Frontera, S. K. Pandey, *New J. Chem.* **2021**, *45*, 19402; c) C. Basak, R. M. Gomila, A. Frontera, S. Chattopadhyay, *CrystEngComm* **2021**, *23*, 2703–2710.
[20] a) F. Weigend, M. Häser, *Theor. Chem. Acc.* **1997**, *97*, 331–340; b) F. Weigend, R. Ahlrichs, *Phys. Chem. Chem. Phys.* **2005**, *7*, 3297–3305.
[21] R. Ahlrichs, M. Bar, M. Haser, H. Horn, C. Kolmel, *Chem. Phys. Lett.* **1989**, *162*, 165–169.
[22] A. D. Becke, *Phys. Rev. A* **1988**, *38*, 3098–3100.
[23] S. Grimme, J. Antony, S. Ehrlich, H. Krieg, *J. Chem. Phys.* **2010**, *132*, 154104.
[24] AIMAll, T. A. Keith, TK Gristmill Software, Overland Park KS, USA, **2019**, (aim.tkgristmill.com).
[25] a) A. D. Becke, *J. Chem. Phys.* **1993**, *98*, 5648–5652; b) P. J. Stephens, F. J. Devlin, C. F. Chabalowski, M. J. Frisch, *J. Phys. Chem.* **1994**, *98*, 11623–11627.
[26] Gaussian 16, Revision B.01, M. J. Frisch, G. W. Trucks, H. B. Schlegel, G. E. Scuseria, M. A. Robb, J. R. Cheeseman, G. Scalmani, V. Barone, G. A. Petersson, H. Nakatsuji, X. Li, M. Caricato, A. V. Marenich, J. Bloino, B. G. Janesko, R. Gomperts, B. Mennucci, H. P. Hratchian, J. V. Ortiz, A. F. Izmaylov, J. L. Sonnenberg, D. Williams-Young, F. Ding, F. Lipparini, F. Egidi, J. Goings, B. Peng, A. Petrone, T. Henderson, D. Ranasinghe, V. G. Zakrzewski, J. Gao, N. Rega, G. Zheng, W. Liang, M. Hada, M. Ehara, K. Toyota, R. Fukuda, J. Hasegawa, M. Ishida, T. Nakajima, Y. Honda, O. Kitao, H. Nakai, T. Vreven, K. Throssell, J. A. Montgomery, Jr., J. E. Peralta, F. Ogliaro, M. J. Bearpark, J. J. Heyd, E. N. Brothers, K. N. Kudin, V. N. Staroverov, T. A. Keith, R. Kobayashi, J. Normand, K. Raghavachari, A. P. Rendell, J. C. Burant, S. S. Iyengar, J. Tomasi, M. Cossi, J. M. Millam, M. Klene, C. Adamo, R. Cammi, J. W. Ochterski, R. L. Martin, K. Morokuma, O. Farkas, J. B. Foresman, D. J. Fox, Gaussian, Inc., Wallingford CT, **2016**.
[27] F. Weinhold, C. R. Landis, E. D. Glendening, *Int. Rev. Phys. Chem.* **2016**, *35*, 399–440.

Manuscript received: May 30, 2022
Accepted manuscript online: June 7, 2022
Version of record online: July 13, 2022